3. D. Ford *et al.*, *Am. J. Hum. Genet.* **62**, 676 (1998).
4. E. Levy-Lahad *et al.*, *Am. J. Hum. Genet.* **60**, 1059 (1997).
5. J. P. Struewing *et al.*, *N. Engl. J. Med.* **336**, 1401 (1997).
6. F. H. Fodor *et al.*, *Am. J. Hum. Genet.* **63**, 45 (1998).
7. S. Thorlacius *et al.*, *Lancet* **352**, 1337 (1998).
8. E. Warner *et al.*, *J. Natl. Cancer Inst.* **91**, 1241 (1999).
9. J. L. Hopper *et al.*, *Cancer Epid. Biomark. Prev.* **8**, 741 (1999).
10. Anglian Breast Cancer Study Group, *Br. J. Cancer* **83**, 1301 (2000).
11. H. A. Risch *et al.*, *Am. J. Hum. Genet.* **68**, 700 (2001).
12. J. M. Satagopan *et al.*, *Cancer Epid. Biomark. Prev.* **10**, 467 (2001).
13. W. D. Foulkes, J. S. Brunet, N. Wong, J. Goffin, P. O. Chappuis, *J. Med. Genet.* **39**, 407 (2002).
14. M. S. Brose *et al.*, *J. Natl. Cancer Inst.* **94**, 1365 (2002).
15. J. M. Satagopan *et al.*, *Clin. Cancer Res.* **8**, 3776 (2002).
16. A. Antoniou *et al.*, *Am. J. Hum. Genet.* **72**, 1117 (2003).
17. Materials and methods are available as supporting material on *Science* Online.
18. C. Oddoux *et al.*, *Nat. Genet.* **14**, 188 (1996).
19. T. S. Frank *et al.*, *J. Clin. Oncol.* **20**, 1480 (2002).
20. J. D. Kalbfleisch, R. L. Prentice, *The Statistical Analysis of Failure Time Data* (Wiley, New York, 1980).
21. C. B. Begg, *J. Natl. Cancer Inst.* **94**, 1221 (2002).
22. G. A. Colditz, B. A. Rosner, F. Speizer, *J. Natl. Cancer Inst.* **88**, 365 (1996).
23. C. L. Carpenter, R. K. Ross, A. Paganini-Hill, L. Bernstein, *Int. J. Cancer* **106**, 96 (2003).
24. L. Scheuer *et al.*, *J. Clin. Oncol.* **20**, 1260 (2002).
25. N. D. Kauff *et al.*, *N. Engl. J. Med.* **346**, 1609 (2002).
26. T. R. Rebbeck *et al.*, *N. Engl. J. Med.* **346**, 1616 (2002).
27. L. C. Hartmann *et al.*, *J. Natl. Cancer Inst.* **93**, 1633 (2001).
28. H. Meijers-Heijboer *et al.*, *N. Engl. J. Med.* **345**, 159 (2001).

29. This project was supported by the Breast Cancer Research Foundation and by the Department of Defense Breast Cancer Research Program (project 17-98-18257). We especially thank E. Lauder for ongoing support. The authors are grateful to the more than 100 graduate students of the Human Genetics Program at Sarah Lawrence College who were instrumental in bringing this project to fruition.

Supporting Online Material

www.sciencemag.org/cgi/content/full/302/5645/643/DC1
Materials and Methods
SOM Text
Tables S1 to S3
References

3 July 2003; accepted 8 September 2003

Structure of Rab GDP-Dissociation Inhibitor in Complex with Prenylated YPT1 GTPase

Alexey Rak,[1] Olena Pylypenko,[3] Thomas Durek,[1] Anja Watzke,[2] Susanna Kushnir,[1] Lucas Brunsveld,[2] Herbert Waldmann,[2,4] Roger S. Goody,[1] Kirill Alexandrov[1]*

Rab/Ypt guanosine triphosphatases (GTPases) represent a family of key membrane traffic regulators in eukaryotic cells whose function is governed by the guanosine diphosphate (GDP) dissociation inhibitor (RabGDI). Using a combination of chemical synthesis and protein engineering, we generated and crystallized the monoprenylated Ypt1:RabGDI complex. The structure of the complex was solved to 1.5 angstrom resolution and provides a structural basis for the ability of RabGDI to inhibit the release of nucleotide by Rab proteins. Isoprenoid binding requires a conformational change that opens a cavity in the hydrophobic core of its domain II. Analysis of the structure provides a molecular basis for understanding a RabGDI mutant that causes mental retardation in humans.

Rab/Ypt proteins, the largest subgroup of the Ras GTPase superfamily, function as molecular switches mediating tethering, docking, fusion, and motility of intracellular membranes (*1*). The multitude of Rab-controlled processes is reflected in the occurrence of a large number of predominately structurally unrelated Rab-interacting proteins (*2*, *3*). However, the Rab escort protein (REP) and the Rab GDP-dissociation inhibitor (RabGDI), which form the family of RabGDI/REP proteins, are shared by all known Rab proteins. RabGDI is a key regulator of Rab/Ypt GTPases that controls the distribution of the active GTP and inactive GDP-bound forms between membranes and cytosol (*4*). RabGDI can deliver to and retrieve from the membrane only Rab/Ypt proteins that are both geranylgeranylated and GDP loaded. A RabGDI deletion is lethal in yeast, whereas the I92P mutation (*5*) in the α-*RabGDI* gene leads to X-linked nonsyndromic mental retardation in humans (*6*, *7*).

The structure of RabGDI solved previously revealed a molecule composed of two domains tilted with respect to each other (*8*). Mutational analysis defined the region of the molecule involved in the association with Rab proteins (Rab-binding platform) and a putative membrane receptor–interacting region termed the mobile effector loop (MEL) (*4*). However, the structure of α-RabGDI reveals neither the position of the lipid-binding site nor the mechanism of GDP-dissociation inhibition or Rab membrane delivery and extraction (*4*). Recently, a structure of the mammalian α-RabGDI in complex with geranylgeranyl cysteine was solved, which led to the suggestion that the lipid-binding site is located on domain I above the MEL (*9*).

Attempts to determine the structure of the Rab:RabGDI complex have been hampered by technical problems: First, overexpression of RabGTPases in eukaryotic expression systems results in only a minor fraction of prenylated RabGTPase bound to membranes, which precludes production of large amounts

Table 1. Statistics of diffraction data collection and refinement. The x-ray source was SLS, Villingen. The detector was a MARCCD (charge-coupled device). Completeness, R_{sym}, and $I/\sigma(I)$ are given for all data and for the highest resolution shell: 1.6 to 1.5 Å. The model was from the Protein Data Bank, PDB ID 1GND. The structure was solved by molecular replacement method using the crystallography and NMR system of ref. (*26*). Abbreviations: mc/sc/lig/wat, main chain, side chain, ligand (GDP, geranylgeranyl), water molecules.

Parameter	Value
Data collection	
Wavelength (Å)	0.9803
Resolution (Å)	19.5–1.5
R_{sym}* (last shell)	7 (40.5)
Observations total/unique	392839/106322
Completeness (last shell)	98.4 (96.3)
$\langle I\rangle/\sigma(I)$ (last shell)	11.6 (3.1)
Molecular replacement model	Bovine α-RabGDI
Refinement	
Resolution (Å)	19.49–1.5
R_{work}/R_{free}†	19.2/21.6
Protein/GDP/Mg/ geranylgeranyl/ water atoms	5100/28/1/20/911
Included amino acids,	
RabGDI	5–446
YPT1	3–198, 206
RMSD bonds/angles (Å/degree)	0.011/1.6
B (Å^2) (mc/sc/lig/wat)	13.3/16.2/7.4, 34.4/26.4

*$R_{sym} = \Sigma_j|I_j - \langle I_j\rangle|/\Sigma_j I_j$, where $\langle I_j\rangle$ is the average intensity of reflection j for its symmetry equivalents; values in parentheses are for the highest resolution shell. †$R_{work} = \Sigma||F_{obs}| - k|F_{calc}||/\Sigma|F_{obs}|$. Five percent of randomly chosen reflections were used for the calculation of R_{free}.

[1]Department of Physical Biochemistry and [2]Department of Chemical Biology, Max-Planck-Institute for Molecular Physiology, Otto-Hahn-Strasse 11, 44227 Dortmund, Germany. [3]Department of Biomolecular Mechanisms, Max-Planck-Institut for Medical Research, Jahnstrasse 29, 69120 Heidelberg, Germany. [4]Department of Organic Chemistry, University of Dortmund, Otto-Hahn-Strasse 6, 44227 Dortmund, Germany.

*To whom correspondence should be addressed. E-mail: kirill.alexandrov@mpi-dortmund.mpg.de

of modified proteins (*10*). Second, in vitro prenylation with recombinant Rab geranylgeranyltransferase results in prenylated Rab proteins that cannot be easily separated from their molecular chaperone REP (*11*). To circumvent these problems, we developed an approach that combines recombinant-protein production, chemical synthesis of lipidated peptides with precisely designed and readily alterable structures, and a technique for peptide-to-protein ligation. As shown here, a truncated version of the Ypt1 protein lacking two amino acids was expressed in *Escherichia coli* in fusion with an intein domain, which then was cleaved off during purification to yield a thioester-tagged GTPase (fig. S1). A synthetic dipeptide, Cys-Cys(geranylgeranyl), mimicking the missing C-terminal residues of Ypt1, was produced by using both solid- and solution-phase techniques (*12*, *13*). The expressed protein ligation (EPL) method was used to join the fragments with a native peptide bond (*14*). The protein was complexed to recombinant yeast RabGDI and purified by gel filtration. Crystals were obtained under the conditions described in the supporting online materials, and the diffraction data were collected to 1.5 Å resolution (Table 1). Initial x-ray phases were obtained by molecular replacement using the coordinates of α-RabGDI [Protein Databank (PDB) code 1GND] as a search model. Cyclic rounds of model building and refinement resulted in a 1.5 Å resolution model of the Ypt1:RabGDI complex that has good values for stereochemistry and crystallographic validation parameters (Table 1 and table S1).

The Ypt1:RabGDI complex has a roughly cylindrical shape, with an extensive interface of ~1880 Å^2 area (Fig. 1A). The structure of yeast RabGDI has a root mean square deviation (RMSD) on Cα of 1.9 Å compared with the structure of mammalian α-RabGDI, with the major changes involving a rigid body shift of helices I, C, and B of domain I and helix D of domain II (fig. S3A). The structure of uncomplexed Ypt1:GDP is not yet known, but Ypt1:GDP from the complex superimposes with the uncomplexed of Ypt7:GDP with a Cα RMSD of 1.8 Å (*15*) (fig. S3B). The most significant change is a break in the C-terminal α helix 5, where a 120° turn directs the rest of the C-terminus toward the effector loop of RabGDI (Fig. 2A). Contact between the molecules is established through a combination of polar and hydrophobic interactions and involves the switch I and II regions and the C-terminus of Ypt1, including the geranylgeranyl moiety on yC206 (y, on Ypt1) (Fig. 2A and fig. S2). The RabGDI molecule contacts Ypt1 primarily via the Rab-binding platform and β strands e1 and e3 and helix C, which form a separate binding site. We term the latter the C-terminus–binding region (CBR), which appears to be an essential structural element, forming a number of interactions with the C-terminus and switch I of Ypt1. The lipid-binding site is formed by helices D, E, H, and F of domain II (Fig. 1 and Fig. 2, B and C). Additional minor contacts involve the N- and C-termini, as well as the MEL. The majority of Rab-binding platform residues involved in hydrogen bond formation with Ypt1 are invariable throughout the RabGDI/REP family (fig. S2). Three additional invariable residues are located on the CBR and form hydrogen bonds with the switch I region and the C-terminus of Ypt1 (fig. S2). Of note, the residues involved in hydrophobic and polar interactions show quite a different distribution on the RabGDI:Ypt interface. Only two of the hydrophobic contacts are located on the Rab-binding platform and interact with the switch I and II regions of Ypt1. Most of the residues forming hydrophobic interactions are clustered on the CBR and the effector loop and are involved in interaction with the C-terminus of Ypt1 (Fig. 2A and fig. S2). The asymmetric distribution of polar and hydrophobic residues on the RabGDI:Ypt1 interface is probably enforced by the distribution of conserved residues through Rab/Ypt molecules. The central

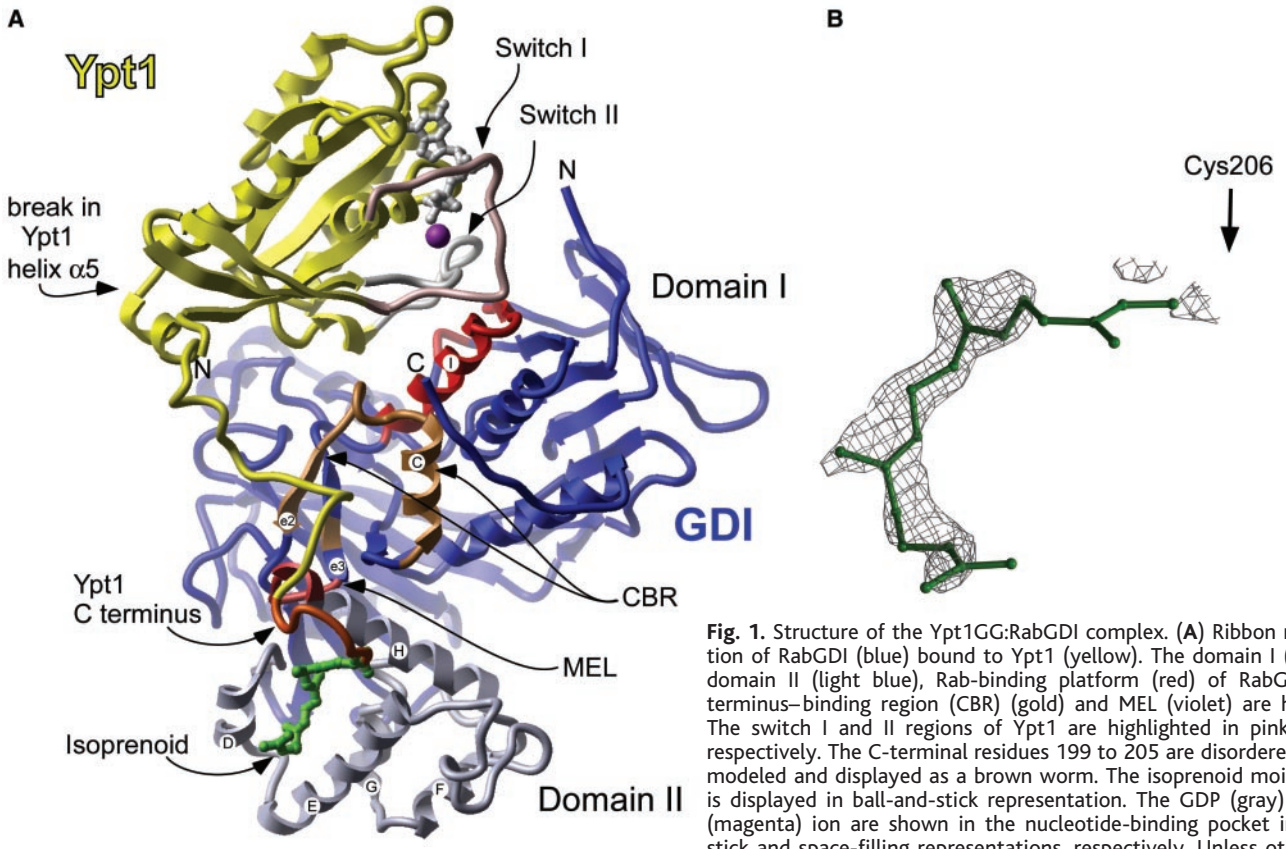

Fig. 1. Structure of the Ypt1GG:RabGDI complex. (**A**) Ribbon representation of RabGDI (blue) bound to Ypt1 (yellow). The domain I (dark blue), domain II (light blue), Rab-binding platform (red) of RabGDI, the C-terminus–binding region (CBR) (gold) and MEL (violet) are highlighted. The switch I and II regions of Ypt1 are highlighted in pink and gray, respectively. The C-terminal residues 199 to 205 are disordered and were modeled and displayed as a brown worm. The isoprenoid moiety (green) is displayed in ball-and-stick representation. The GDP (gray) and Mg^{2+} (magenta) ion are shown in the nucleotide-binding pocket in ball-and-stick and space-filling representations, respectively. Unless otherwise indicated, this and other figures were prepared using ICM (Molsoft LLC) (**B**) A view of the final $2(F_{obs} - F_{calc})$ map, contoured at 1.0 σ covering geranylgeranyl lipid. An arrow denotes the protein-conjugated end of the lipid. The picture was generated with BobScript and PovRay.

part of the molecule harboring the nucleotide-binding site is highly conserved throughout the entire subfamily of RabGTPases, whereas the C-terminal portions are hypervariable and are believed to determine the organelle specificity of Rab molecules (*16*). However, it is expected that the C-terminus of Rab molecules must be located in the vicinity of the MEL that is necessary for interaction with target membranes. In order to accommodate the highly divergent C-terminal sequences, RabGDI:Rab complexes appear to rely on either hydrophobic interactions that require a much lower degree of side-chain conservation or on polar interactions involving main chain atoms of the Ypt/Rab C-terminus. Ypt1 contacts RabGDI primarily via a dense network of hydrogen bonds formed by the switch II and switch I regions. Several invariable residues of the Rab family, such as these on Ypt1, yR69, yR79, yQ67, yD63, and yD44, make up the core of these interactions. The last two mentioned appear to be key elements of the RabGDI-mediated inhibition of nucleotide release by RabGTPase.

One of the challenges in the membrane transport field has been to understand the molecular basis of RabGDI/REP family members' selectivity for the GDP-bound form of Rab GTPase, as well as to determine how they sequester Rab-conjugated geranylgeranyl groups. One of the most obvious consequences of Ypt1 interaction with RabGDI is the increased rigidity of the switch I and II regions as determined by the presence of interpretable electron density for these re-

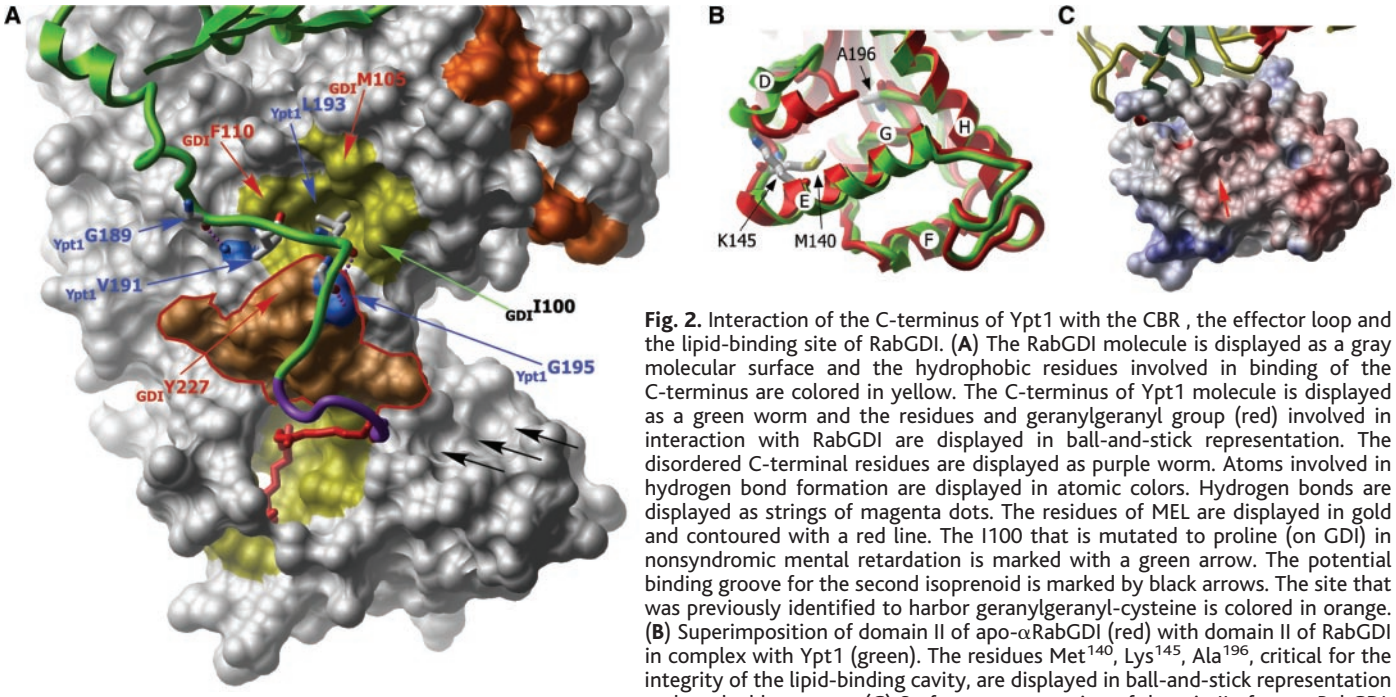

Fig. 2. Interaction of the C-terminus of Ypt1 with the CBR , the effector loop and the lipid-binding site of RabGDI. (**A**) The RabGDI molecule is displayed as a gray molecular surface and the hydrophobic residues involved in binding of the C-terminus are colored in yellow. The C-terminus of Ypt1 molecule is displayed as a green worm and the residues and geranylgeranyl group (red) involved in interaction with RabGDI are displayed in ball-and-stick representation. The disordered C-terminal residues are displayed as purple worm. Atoms involved in hydrogen bond formation are displayed in atomic colors. Hydrogen bonds are displayed as strings of magenta dots. The residues of MEL are displayed in gold and contoured with a red line. The I100 that is mutated to proline (on GDI) in nonsyndromic mental retardation is marked with a green arrow. The potential binding groove for the second isoprenoid is marked by black arrows. The site that was previously identified to harbor geranylgeranyl-cysteine is colored in orange. (**B**) Superimposition of domain II of apo-αRabGDI (red) with domain II of RabGDI in complex with Ypt1 (green). The residues Met^{140}, Lys^{145}, Ala^{196}, critical for the integrity of the lipid-binding cavity, are displayed in ball-and-stick representation and marked by arrows. (**C**) Surface representation of domain II of apo-αRabGDI. The surface is colored according to charge, and position of lipid-binding cavity is denoted by a red arrow.

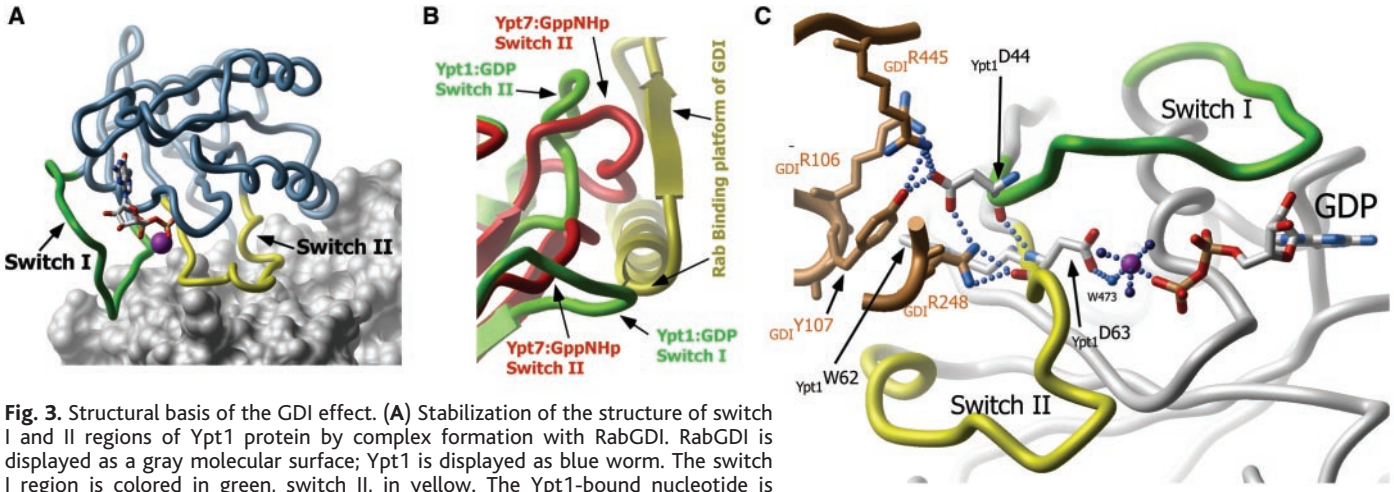

Fig. 3. Structural basis of the GDI effect. (**A**) Stabilization of the structure of switch I and II regions of Ypt1 protein by complex formation with RabGDI. RabGDI is displayed as a gray molecular surface; Ypt1 is displayed as blue worm. The switch I region is colored in green, switch II, in yellow. The Ypt1-bound nucleotide is displayed in ball-and-stick representation in atomic colors; the Mg^{2+} ion is displayed as magenta ball. (**B**) Superimposition of the nonhydrolyzable analog of GTP Ypt7GppNHP (red ribbon) with Ypt1:GDP (green ribbon) in complex with RabGDI (yellow ribbon). (**C**) Interaction of the residues of the RabGDI Rab-binding platform with residue $yAsp^{63}$ ($_{Ypt1}$D63) involves water-mediated interaction with the Mg^{2+} ion. Elements of the Rab-binding platform of RabGDI are displayed in worm representation (gold); the interacting residues are displayed in ball-and-stick representation. Ypt1 is displayed as a gray worm with the interacting residues in ball-and-stick representation (white and atomic colors), the switch regions are colored as in (A). Water molecules are displayed as blue balls and the Mg^{2+} ion is shown as a magenta ball. The GDP is displayed as ball-and-stick in atomic colors. The potential hydrogen bonds are displayed as strings of blue balls.

gions and their low *B* factors (fig. S3B). Ras-like GTPases and, in particular, Rab proteins display high flexibility in these regions, and the switch regions of uncomplexed Ypt7 and Rab7 are largely disordered (*15*, *17*). Thus, stabilization of the switch regions is expected to provide an additional obstacle for nucleotide release by GTPases (Fig. 2A). Regulatory factors that stimulate nucleotide exchange interact with the switch regions and, in the case of the SOS:H-Ras interaction, were demonstrated to fix switch I region in an open conformation, which promotes nucleotide release (*18*). From this perspective, exchange factors and RabGDI use similar mechanisms to exert the control over the GTPase nucleotide-bound state by stabilizing the switch regions in open or closed conformations, respectively.

More localized interactions may also contribute to the affinity increase for GDP. As can be seen in fig. S2 and Fig. 2C, several residues of RabGDI establish contacts with residues of the switch I and II regions in the vicinity of the phosphate groups of GDP. In particular, gR248 (g, on GDI) forms a hydrogen bond with the main chain oxygen of yD63. This residue is conserved throughout the Ras superfamily and coordinates one of four water molecules arranged around the Mg^{2+} ion in the GDP state. The Mg^{2+} ion is important for both nucleotide binding and hydrolysis. It appears that hydrogen bond formation between gR248 and yD63 stabilizes the coordination of Mg^{2+} via water molecule 473 and thus reduces the rate of GDP release.

In order to understand the selectivity of RabGDI for the GDP-bound form of GTPases, we superimposed the structure of the Ypt7:GppNHp (*15*) with the Ypt1(GDP):RabGDI complex. This yielded an RMSD of all Cα atoms of 1.9 Å. The only significant differences are located in switch I and II (Fig. 3B). The switch I and II region of the GTP-bound conformation would clash with residues of the Rab-binding platform and thus would reduce the affinity of the interaction with RabGDI. This provides a mechanism for the nucleotide-dependent recognition of Rab/Ypt proteins by members of the RabGDI/REP family that can be compared with the mechanism of Cdc42:RhoGDI interaction (*19*). In the latter case, the GDI effect also depends on the enhanced coordination of the Mg^{2+} ion. However, this does not involve the Mg^{2+}-clustered water molecules but the Thr^{35} residue on Cdc42 of the switch I region that directly mediates the contact between the regulatory arm of RhoGDI and the nucleotide-associated Mg^{2+} ion. Moreover, the structure of the switch II region of Cdc42 is not influenced by complex formation, and the complex can accommodate both nucleotide-bound forms of RhoGTPase. Thus, it appears that, in general, GDI molecules use the switch regions of small GTPases to inhibit nucleotide dissociation, but the specific mechanisms can differ considerably.

The location of the lipid-binding site on the RabGDI molecule has been a long-standing question. The determination of the structures of α-RabGDI and REP-1 did not reveal a hydrophobic patch on the surface sufficiently large to harbor two geranylgeranyl moieties (*8*, *9*, *20*). Unexpectedly, in the complex reported here, the geranylgeranyl lipid is not associated with the previously suggested binding site but instead is buried in a deep cavity in domain II (Figs. 1 and 2A; Movie S1). The walls of the cavity are formed by α helices D, E, and H; the back is blocked by helix F and β strand b2 of domain II. The inner surface of the cavity is lined by nonpolar residues that provide a hydrophobic environment for the conjugated isoprenoid. Superimposition of the structure of apo-αRabGDI with the structure of the complex demonstrates that the cavity emerges as a consequence of the outward movement of helix D, whereas the rest of domain II adopts a very similar conformation in both mammalian and yeast RabGDI (fig. S3A). Therefore, it appears that a conformational change provides access for the lipid to the hydrophobic core of domain II. At least three independent lines of evidence support this observation. First, replacement of the invariant residue Ala^{187} by Val (on GDI) leads to developmental defects in *Drosophila* (*21*). This residue is located at the bottom of the identified lipid-binding site, and its substitution would make the binding cavity shallower. Second, mutation M140I reduces the ability of yeast RabGDI to extract Ypt proteins from intracellular membranes (*22*). On the basis of the structure, this mutation is also expected to change the geometry of the binding site (Fig. 2A). Third, analysis of the structure of the lipid-binding cavity suggests that gK145 may play an important role in formation of the lipid-binding cavity by functioning as a spreader that keeps helices D and E apart (Fig. 3B). Consistent with this proposal, the K145A mutation almost completely inhibited the ability of RabGDI to extract Ypt1 from yeast membranes (fig. S4). Together, these data suggest that the identified cavity is indeed involved in extraction of Rab/Ypt proteins from the membrane.

The identified lipid-binding site is too small to accommodate two conjugated isoprenoids, which raises the question of the possible position of the second lipid. Two conjugated isoprenoids buried in the hydrophobic core might be too difficult to extract for the transfer into the lipid bilayer. Thus, we suggest that the lipid is likely to be accommodated outside the cavity, possibly in the adjacent groove (Fig. 2A). The

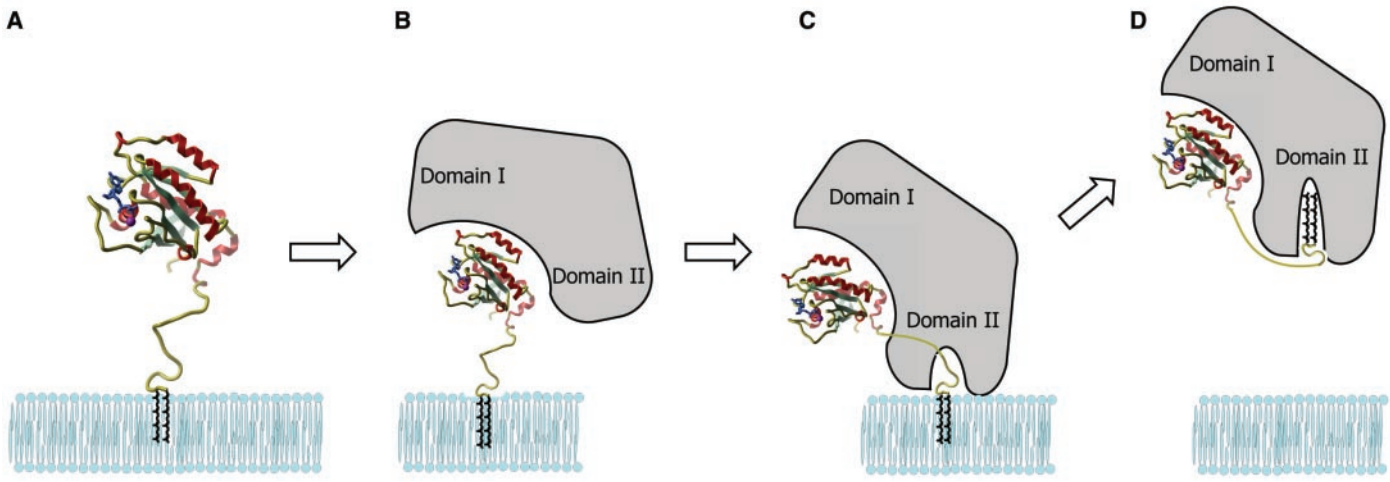

Fig. 4. Model for RabGDI-mediated Ypt1 interaction with the membrane. (**A**) Model for the initial recognition of the membrane associated Rab/Ypt GTPase by RabGDI. (**B**) Interaction of RabGDI with the nucleotide-binding domain and C-terminus of membrane-bound Rab/Ypt GTPase and its positioning in the vicinity of the membrane-buried isoprenoids and initiation of the conformational change in the domain II. (**C**) Formation of an isoprenoid-binding cavity on the domain II of RabGDI and solubilization of Rab/Ypt GTPase. (**D**) Formation of soluble RabGDI:Rab complex.

fact that monoprenylated Rab:REP complexes appear to be more stable than the diprenylated species indirectly supports this assumption (*23*).

The structure provides a basis for analysis of disease-causing mutations in RabGDI, such as I100P (I92P in mammalian nomenclature), which leads to familial mental retardation in humans. This mutation is characterized by reduced Rab extraction from the membranes (*7*). gI100 is located in the CBR and is part of a group of nonpolar residues on the surface of the RabGDI molecule that form an extended hydrophobic patch with a central cavity on the lower part of domain II (Fig. 2A). This assembly is involved in binding of the C-terminus of Ypt1 via interaction with Val^{191} and Leu^{193} and induces a 90° turn in the C-terminus, which directs it over the effector loop toward the lipid-binding site. Mutations in this hydrophobic patch are expected to have a twofold effect. First, they will impair C-terminus binding and will reduce the affinity of the RabGDI molecule for Ypt. Second, and possibly more important, they will perturb the orientation of the Ypt C-terminus in the vicinity of the effector loop and the lipid-binding domain. This is likely to interfere with GTPase interaction with molecules assisting delivery and removal of Rab proteins to and from the membrane. Consistent with this model, mutations in residues Thr^{105} and Tyr^{227}, which are part of the same hydrophobic patch, were also shown to interfere with membrane extraction of Ypt/Rab proteins (*22*, *24*). Therefore, the α-RabGDI mutation I92P associated with mental retardation compromises the interaction with the peptide part of the C-terminus, and not the integrity of the isoprenoid-binding site, as initially proposed (*9*).

The structure also provides additional insights into the mechanism of RabGDI-mediated delivery of Rab proteins to the membranes. At least three structural elements of the complex were proposed to regulate loading of Rab proteins onto membranes: the hypervariable region of the Rab C-terminus, the conjugated isoprenoids, and the effector loop of RabGDI (*4*, *16*, *25*). All these elements are closely associated and well exposed in the Ypt1:RabGDI complex, making them clearly accessible to the putative membrane receptor (Figs. 1A and 2A).

In summary, we suggest a model in which RabGDI initially recognizes the globular core domain of the Rab/Ypt molecule by the Rab-binding platform interaction with switch I and II regions. This relatively low affinity binding is followed by interaction of the initially disordered C-terminus with the hydrophobic patch of the CBR. This stabilizes the interaction of domain II of RabGDI with the membrane over the buried geranylgeranyl moieties. A conformational change leads to opening of the hydrophobic cavity between helixes D and E in domain II and facilitates extraction of the first geranylgeranyl lipid from the bilayer (Fig. 4). The second lipid follows and is accommodated in the vicinity of the first lipid-binding site. This mechanism helps to explain the detrimental effect of mutations leading to weaker binding of the Rab C-terminus.

Reference and Notes

1. S. R. Pfeffer, *Trends Cell Biol.* **11**, 487 (2001).
2. N. Segev, *Curr. Opin. Cell Biol.* **13**, 500 (2001).
3. M. Zerial, H. McBride, *Nature Rev. Mol. Cell Biol.* **2**, 107 (2001).
4. C. Alory, W. E. Balch, *Traffic* **2**, 532 (2001).
5. In the protein, Ile^{92} is replaced by Pro (I92P). Single-letter abbreviations for the amino acid residues are as follows: A, Ala; C, Cys; D, Asp; E, Glu; F, Phe; G, Gly; H, His; I, Ile; K, Lys; L, Leu; M, Met; N, Asn; P, Pro; Q, Gln; R, Arg; S, Ser; T, Thr; V, Val; W, Trp; and Y, Tyr.
6. M. D. Garrett, J. E. Zahner, C. M. Cheney, P. J. Novick, *EMBO J.* **13**, 1718 (1994).
7. P. D'Adamo *et al.*, *Nature Genet.* **19**, 134 (1998).
8. I. Schalk *et al.*, *Nature* **381**, 42 (1996).
9. Y. An *et al.*, *Structure* (*Cambridge*) **11**, 347 (2003).
10. H. Horiuchi, O. Ullrich, C. Bucci, M. Zerial, *Methods Enzymol.* **257**, 9 (1995).
11. A. Kalinin *et al.*, *Protein Expr. Purif.* **22**, 84 (2001).
12. K. Alexandrov *et al.*, *J. Am. Chem. Soc.* **124**, 5648 (2002).
13. B. Ludolph, F. Eisele, M. Waldeman, *J. Am. Chem. Soc.* **124**, 5954 (2002).
14. T. W. Muir, *Annu. Rev. Biochem.* **72**, 249 (2003).
15. A. T. Constantinescu *et al.*, *Structure* (*Cambridge*) **10**, 569 (2002).
16. P. Chavrier *et al.*, *Nature* **353**, 769 (1991).
17. A. Rak, K. Alexandrov, unpublished observations.
18. P. A. Boriack-Sjodin, S. M. Margarit, D. Bar-Sagi, J. Kuriyan, *Nature* **394**, 337 (1998).
19. G. R. Hoffman, N. Nassar, R. A. Cerione, *Cell* **100**, 345 (2000).
20. O. Pylypenko *et al.*, *Mol. Cell* **11**, 483 (2003).
21. C. S. Ricard *et al.*, *Genesis* **31**, 17 (2001).
22. P. M. Gilbert, C. G. Burd, *J. Biol. Chem.* **276**, 8014 (2001).
23. F. Shen, M. C. Seabra, *J. Biol. Chem.* **271**, 3692 (1996).
24. T. Sakisaka, T. Meerlo, J. Matteson, H. Plutner, W. E. Balch, *EMBO J.* **21**, 6125 (2002).
25. P. Luan *et al.*, *Traffic* **1**, 270 (2000).
26. A. T. Brunger *et al.*, *Acta Crystallogr. D Biol. Crystallogr.* **54** (Pt. 5), 905 (1998).

27. G. Holtermann is acknowledged for invaluable technical assistance. We thank the staff of SLS beamline at Paul Scherrer Institute, Villingen, for help during data collection. We thank I. Schlichting and W. Blankenfeldt for help with data collection and A.-C. Ceacareanu for help with construction of expression vectors. D. Gallwitz is acknowledged for a generous gift of anti-Ypt1 antibody. W. Blankenfeldt is gratefully acknowledged for critically reading the manuscript and stimulating discussions. A.R. was supported by an Engelhorn foundation long-term postdoctoral fellowship. L.B. was supported by postdoctoral fellowship of the Alexander von Humboldt Foundation. This work was supported in part by grant DFG AL 484/5-2 to K.A. and grant I/77 977 of the Volkswagen foundation to K.A., R.S.G., and H.W. Coordinates have been deposited in the Protein Data Bank (Brookhaven National Laboratory) with accession number 1URV.

Supporting Online Material

www.sciencemag.org/cgi/content/full/302/5645/646/DC1
Materials and Methods
Figs. S1 to S3
Table S1
References and Notes
Movie S1

9 June 2003; accepted 5 September 2003

A New Class of Bacterial RNA Polymerase Inhibitor Affects Nucleotide Addition

Irina Artsimovitch,[1]* Clement Chu,[2] A. Simon Lynch,[2]† Robert Landick[1]†

RNA polymerase (RNAP) is the central enzyme of gene expression. Despite availability of crystal structures, details of its nucleotide addition cycle remain obscure. We describe bacterial RNAP inhibitors (the CBR703 series) whose properties illuminate this mechanism. These compounds inhibit known catalytic activities of RNAP (nucleotide addition, pyrophosphorolysis, and Gre-stimulated transcript cleavage) but not translocation of RNA or DNA when translocation is uncoupled from catalysis. CBR703-resistance substitutions occur on an outside surface of RNAP opposite its internal active site. We propose that CBR703 compounds inhibit nucleotide addition allosterically by hindering movements of active site structures that are linked to the CBR703 binding site through a bridge helix.

Bacterial RNAPs typically consist of five polypeptides: β,′β, α, and ω. β′ and β form a main channel that holds the RNA 3′ OH in the active site, an 8 to 9 base pair RNA:DNA hybrid, duplex DNA in front of the hybrid, and single-stranded RNA upstream from the hybrid. A secondary channel connects the active site to the surrounding solution and may serve as a passageway for entering nucleoside triphosphates (NTPs), exiting pyrophosphate, or both. Within the main channel, bacterial and eukaryotic RNAPs are nearly identical in structure; thus, the mechanism of transcription by the multisubunit RNAPs of

[1]Department of Bacteriology, University of Wisconsin, Madison, WI 53706, USA. [2]Cumbre Inc., 1502 Viceroy Drive, Dallas, TX 75235, USA.

*Present address: Department of Microbiology, Ohio State University, Columbus, OH 43210, USA.
†To whom correspondence should be addressed. E-mail: simon.lynch@cumbre.net (A.S.L.); landick@bact.wisc.edu (R.L.)